2 (2026) 100013

Contents lists available at ScienceDirect

The EANM Journal

journal homepage: www.sciencedirect.com/journal/the-eanm-journal

Safety, dosimetry and preliminary imaging findings of $[^{68}Ga]$Ga-OncoFAP – a prospective multicenter Phase I clinical trial

Margarita Kirienko [a], Martina Sollini [b,*], Emanuele Balduzzi [c], Alessia Artesani [d,e], Elena Lazzeri [f], Fabrizia Gelardi [b], Francesco Bartoli [g], Andrea Marciano [f], Paola Caroli [h], Samuele Cazzamalli [i], Andrea Galbiati [i], Jacqueline Mock [i], Dario Neri [j], Marco Maccauro [a], Federica Matteucci [h], Pinuccia Faviana [k], Arturo Chiti [b], Paola Anna Erba [b]

[a] Fondazione IRCCS Istituto Nazionale dei Tumori, Milan, Italy
[b] Vita-Salute San Raffaele University, IRCCS Ospedale San Raffaele, Milan, Italy
[c] Department of Medicine and Surgery, University of Milan Bicocca and ASST-Ospedale Papa Giovanni XXIII, Bergamo, Italy
[d] Department of Biomedical Sciences, Humanitas University, v. Levi Montalcini 4, Pieve Emanuele, 20072, Italy
[e] IRCCS Humanitas Research Hospital, v. Manzoni 56, Rozzano, 20089, Italy
[f] Regional Center of Nuclear Medicine, Azienda Ospedaliero Universitaria Pisana, Pisa, Italy
[g] Department of Translational Research and New Technologies in Medicine and Surgery, University of Pisa, Pisa, Italy
[h] IRCCS Istituto Romagnolo per lo Studio dei Tumori "Dino Amadori" - IRST S.r.l., Meldola, Italy
[i] Philochem AG, Otelfingen, Switzerland
[j] Philogen S.p.A., Siena, Italy
[k] Department of Surgical, Medical, Molecular Pathology and Critical Area, University of Pisa, Pisa, Italy

ARTICLE INFO

Keywords:
FAP
PET/CT
Pancreatic cancer
Breast cancer
Esophageal cancer
Colon cancer

ABSTRACT

Background: Fibroblast Activation Protein (FAP) has emerged as a pan-tumoral target for diagnostic and therapeutic radiopharmaceuticals. Gallium-68-labelled OncoFAP ($[^{68}Ga]$Ga-OncoFAP), a small organic radioligand with high affinity for human FAP, has shown promising properties in preclinical experiments. In this prospective Phase I study we aimed to assess the safety, the dosimetry, pharmacokinetics, and preliminary imaging findings of $[^{68}Ga]$Ga-OncoFAP.

Methods: In this multicenter Phase I clinical trial (NCT05784597), patients with breast, esophageal, pancreatic, or colorectal cancer were eligible. After a single administration of 250 (225–275) MBq $[^{68}Ga]$Ga-OncoFAP, we acquired three sets of PET/CT scans (0–30, 60, and 120 min) using ^{68}Ga EARL-accredited scanners. We collected blood and urine samples up to 120 min post injection. Safety was assessed up to 1 week post scan. Adverse events were graded according to Common Terminology Criteria for Adverse Events (CTCAE) v.5. Dosimetry was evaluated centrally. Pharmacokinetics was evaluated based on serial blood samples. Uptake in lesions and healthy organs was evaluated visually and by SUV_{max}, SUV_{mean}, and tumour:organ ratio. Approval from competent authorities and ethics committees was obtained prior to study start.

Results: A total of 18 patients were enrolled. No adverse events related to $[^{68}Ga]$Ga-OncoFAP were recorded. The whole-body effective dose was 16.6–24.6 mSv/GBq (mean 19.9 mSv/GBq, median 19.4 mSv/GBq). The elimination of $[^{68}Ga]$Ga-OncoFAP is predominantly kidney-mediated. All patients showed selective tumor uptake within <10 min after administration (SUV_{max} tumor lesions shortly after injection range 1.99–31.36), which remained stable up to 120 min post injection (SUV_{max} tumor lesions range 5.04–21.7).

Conclusions: $[^{68}Ga]$Ga-OncoFAP was safe and well tolerated. The dosimetry profile is in line with other clinically used radiopharmaceuticals. $[^{68}Ga]$Ga-OncoFAP showed optimal pharmacokinetics with rapid blood clearance and renal excretion. $[^{68}Ga]$Ga-OncoFAP demonstrated promising in PET imaging of a range of solid tumors, providing the rationale for further studies to elucidate its full application.

* Corresponding author. Via Olgettina 60, 20132, Milano, Italy.
E-mail address: sollini.martina@hsr.it (M. Sollini).

https://doi.org/10.1016/j.eanmj.2025.100013
Received 16 September 2025; Received in revised form 3 November 2025; Accepted 26 November 2025
Available online 19 December 2025

List of abbreviations

AE	Adverse Event
AUC	Area under the curve
Cmax	maximum concentration
CT	Computed Tomography
CTCAE	Common Terminology Criteria for Adverse Events
EANM	European Association of Nuclear Medicine
EARL	EANM Research GmbH
ECG	Electrocardiogram
ECOG	Eastern Cooperative Oncology Group
FAP	Fibroblast Activation Protein
FDG	Fluorodeoxyglucose
FWHM	Full Width at Half Maximum
GBq	Gigabecquerel [10^9 s^{-1}]
HCT	hematocrit
IV	intravenous
LLI	Lower Large Intestine
mA	milliampere
MBq	Megabecquerel [10^6 s^{-1}]
mGy	milligrey [10^{-3} J/kg]
mSv	millisievert [10^{-3} J/kg]
NYHA	New York Heart Association
PET	Positron Emission Tomography
PK	Pharmacokinetics
Pts	patients
RMBLR	Red marrow to blood ratio
SD	Standard Deviation
SNMMI	Society of Nuclear Medicine and Molecular Imaging
SUV	Standardized Uptake Value
$t_{1/2}$	half-life
TIA	Time Integrated Activity
ULI	Upper Large Intestine
ULN	Upper Limit of Normal

1. Introduction

Fibroblast Activation Protein (FAP) has emerged as an ideal pan-tumoral marker for the delivery of diagnostic radionuclides. FAP is a membrane-bound endopeptidase that is overexpressed in the stroma of more than 90 % of epithelial cancers including breast, gastrointestinal, and lung cancer [1]. Notably, high FAP expression is observed in many cancer types for which [^{18}F]-fluorodeoxyglucose (FDG) positron emission tomography (PET) and other available imaging modalities offer only suboptimal imaging quality, and which contribute a large proportion of the annual cancer-related deaths [2,3].

The development of FAP-targeting agents began in the late 1980s [4], but interest in these antibodies was initially limited due to challenges related to biodistribution and sensitivity. In 2014, Jansen et al. revitalized interest in FAP-based imaging by introducing a new generation of small-molecule ligands [5]. This first generation of FAP inhibitors (FAPI) has demonstrated the applicability of FAP ligands for imaging of a broad range of cancer types with favorable results [6–8]. A recent systematic review of over 39 studies concluded that the pooled sensitivity of FAP PET/CT on a patient-based analysis was 99 % for the detection of primary tumor lesions, 91 % for nodal, and 99 % for distant metastases. FAP PET/CT was also found to have a higher sensitivity in the detection of primary, nodal, and metastatic lesions based on a paired analysis between FAP PET/CT and [^{18}F]FDG PET/CT [9].

OncoFAP is a recently developed second-generation FAP ligand [10]. One of the advantages of this molecule is that in vivo it shows a very rapid, selective, and high uptake in FAP-expressing tumors and a rapid clearance from the blood and healthy tissues [10,11].

Based on the promising preclinical data and preliminary results in humans from individual patient treatment at the attending physician's discretion [11], a prospective Phase I diagnostic clinical trial of [^{68}Ga]Ga-OncoFAP in patients with breast cancer, colorectal cancer, esophageal cancer, and pancreatic adenocarcinoma was conducted (PH-FAPGA-01/22, NCT 05784597). The primary objectives of the study were to evaluate safety and dosimetry of a single administration of [^{68}Ga]Ga-OncoFAP. In addition, data on the uptake, biodistribution pharmacokinetics (PK), and preliminary PET imaging findings of [^{68}Ga]Ga-OncoFAP were evaluated.

2. Materials and methods

2.1. Study design

A Phase I, multicenter, open-label diagnostic clinical trial was run in four centers in Italy (NCT05784597), in accordance with the Declaration of Helsinki and the International Conference on Harmonisation Good Clinical Practice guidelines. This study was approved by the Ethics Committee Comitato Etico Territoriale Lazio Area 5 (CTIS ID 931, 04/10/2022) and national competent authorities. All patients signed an informed consent form.

Adult patients (18–75 years) with pathologically proven breast cancer, esophageal cancer, colorectal cancer, and pancreatic adenocarcinoma were eligible if they had an indication for staging or restaging, agreed to appropriate contraception. Exclusion criteria included chronically impaired renal function as expressed by creatinine clearance $<$60 mL/min or serum creatinine $>$1.5 x ULN, active hepatitis, significant cardiac disorders (congestive heart failure, NYHA class III-IV, myocardial infarction within one year prior to study entry, uncontrolled hypertension, or arrhythmia), pregnancy or breastfeeding, major trauma including major surgery (such as abdominal/cardiac/thoracic surgery) within 4 weeks of administration of the study drug, serious, non-healing wound, ulcer, or bone fracture as well as any anti-cancer therapy within 3 weeks before [^{68}Ga]Ga-OncoFAP PET/CT scan.

Up to 20 patients were planned to be enrolled into two cohorts (A and B). Cohort A included three (3) female and three (3) male patients with a primary tumor only, while cohort B included up to 14 patients with a primary tumor or metastatic disease with or without primary tumor. Both cohorts were open in parallel, and patients were assigned to the respective cohort according to their disease extent and sex, with a priority for enrolling patients in cohort A, unless the number of patients of a given sex had already been enrolled in cohort A. Safety, pharmacokinetics, and biodistribution were assessed in all patients (Cohort A and B). Dosimetry was evaluated in patients enrolled in Cohort A to assess healthy organs without the interference of uptake by metastatic lesions.

2.2. Radiolabeling and quality controls

OncoFAP-DOTAGA was radiolabeled with ^{68}Ge/^{68}Ga-generator-derived ^{68}Ga at the radiopharmacy of the study centers using a disposable-cassette-based automatic labeling module. The product was then tested for quality to meet the specifications and acceptance criteria. Radiolabelling and quality controls have been performed as previously described [12].

2.3. Study procedures

Patients were scheduled to receive a single intravenous bolus injection of 250 MBq (225–275 MBq) [^{68}Ga]Ga-OncoFAP followed by a series of PET/CT scans. Patients in cohort An underwent a whole-body PET/CT scan immediately after [^{68}Ga]Ga-OncoFAP administration followed by a PET scan at 10 and 20 min post injection. Further whole-body PET/CT scans were acquired at 1 h and 2 h post administration. In addition, blood samples were collected prior to administration and at 1, 3, 5, 7, 10, 15, 30, 45, 60, 75, and 120 min post injection. By contrast, patients enrolled in cohort B underwent a dynamic PET/CT scan from 0 to 30 min post injection over a single bed position covering the main tumor region. At 1 h post administration, a whole-body PET/CT scan was acquired. At 2 h post injection, a 4-min PET/CT scan was performed on the same bed position as the dynamic scan. Blood samples were collected prior to administration, and at 1, 5, 10, 15, 20, 60, and 120 min post injection. In both cohorts, urine samples were collected before administration, at 35–45, 55–60 (optional), 100–120, and 135–150 min post administration. The study procedures are schematically depicted in Fig. 1.

2.4. PET/CT image acquisition and reconstruction

Images were acquired using ^{68}Ga EARL-accredited PET/CT scanners (General Electric Discovery MI, General Electric Discovery 690, General Electric Discovery 710, Siemens Biograph mCT Flow). Low-dose CT was performed using 70–80 mA tube current and 120–140 kVp tube voltage. Image reconstruction was performed applying time-of-flight, iterative reconstruction (21 subsets, 3 iterations using Gaussian Filter, FWHM 4 mm) and corrections for artifacts such as scatter according to site-specific procedures. Images were reconstructed using a 128 × 128 matrix.

2.5. Safety assessment

Safety was assessed based on physical examination, vital signs, ECG, standard laboratory examinations and the collection of adverse events. Adverse events were graded according to the National Cancer Institute Common Terminology Criteria for Adverse Events (CTCAE) version 5.0. These assessments were performed at screening, before the injection of [^{68}Ga]Ga-OncoFAP, after the last PET/CT scan and within 7 days from the administration of [^{68}Ga]Ga-OncoFAP.

2.6. Dosimetry

Dosimetry calculations were performed using OLINDA/EXM 1.0 [13]. Organ delineation at each imaging time point was performed with TotalSegmentator tool [14], an open-source tool able to segment over 117 classes in CT images. To ensure accuracy, all organ delineations were manually reviewed and adjusted as necessary using PLANET® Dose (DOSIsoft) software. The activity was assessed using PLANET® Dose for each organ as segmented on the PET/CT scan. Activity was evaluated only in organs showing radiopharmaceutical uptake. For small organs with low uptake, a robust activity assessment was not feasible. Considering the uptake patterns, activity evaluation was focused on the following organs: brain, small intestine, stomach, heart, kidneys, liver, lungs, pancreas, spleen, and urinary bladder. For organs affected by tumors, the activity of the entire organ was assigned to the remainder of the body and the mean absorbed dose to the organ was not calculated to prevent overestimation in healthy tissues. The average volume of each organ was calculated based on the 3 CT scans acquired and used to derive the custom mass for each organ.

To evaluate the time integrated activity (TIA) for the healthy organs listed above (except urinary bladder) a mono- and bi-exponential fit was performed, and the best fit was chosen according to the Akaike criterion [15]. The TIA and residence time were subsequently calculated for all contoured organs.

The residence time to the urinary bladder was evaluated using the voiding bladder model, calculating pharmaceutical clearance based on a mono-exponential fit of the activity within the patient after excluding excreted urine activity. The actual voiding intervals were personalized for each patient based on the timepoints of urine collection, with an average of approximately 1 h.

The residence time to the red marrow was evaluated by integrating over time the activity concentration in blood after each sampling. For the integration, a trapezoidal fit of the concentration data with a

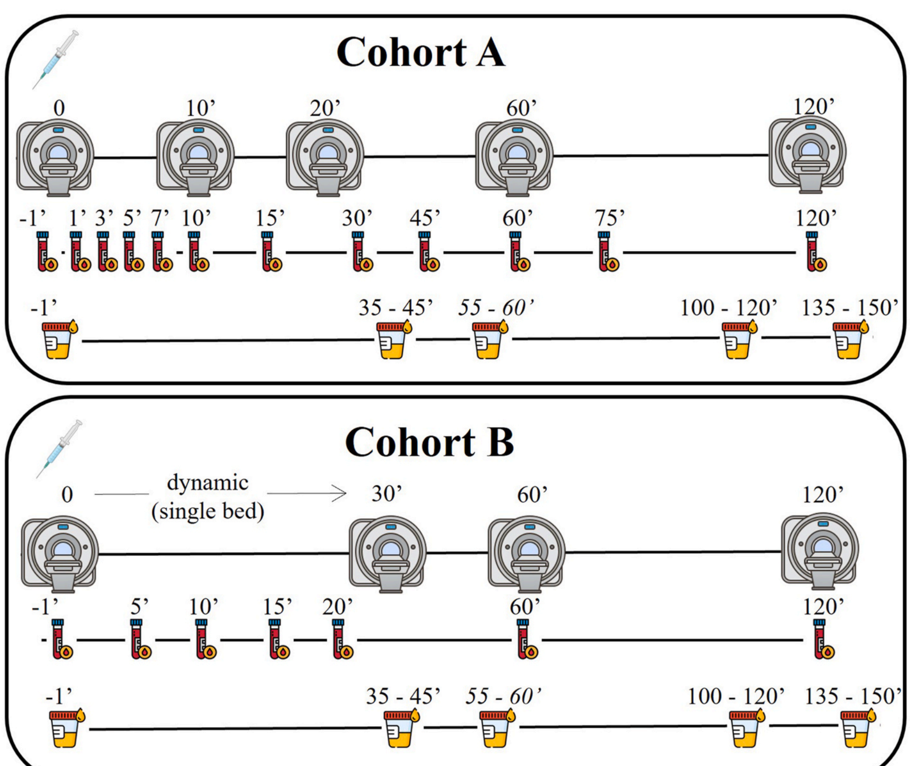

Fig. 1. Schedule of study procedures. Top rows: Timepoints of PET/CT scans. Middle row: Timepoints of blood sampling. Bottom row: Timepoints of urine sampling.

physical decay tail was used. The red marrow-to-blood ratio (RMBLR) was calculated based on the hematocrit values (HCT) of each patient evaluated at screening using the formula RMBLR = 0.19/(1-HCT) [16, 17]. The cumulated activity over time (Ã) was calculated by multiplying the cumulated activity over time per unit volume of the red marrow (Ã/mL) by the average mass of the red marrow (1120 g for men and 1300 g for women [18]).

The remainder of the body activity was defined as total activity injected minus the activity present in healthy organs contoured, red marrow, and urinary bladder. Subsequently, as performed for the healthy organs, the TIA for the remainder of the body was calculated using both mono- and bi-exponential fitting models, with the best fit selected based on the Akaike criterion. The corresponding residence time was then derived accordingly. The mean absorbed dose was calculated based on the residence time and the custom mass using OLINDA/EXM 1.0 [13].

2.7. Pharmacokinetics

Pharmacokinetics of [68Ga]Ga-OncoFAP were analyzed based on serial blood sampling through a catheter in the opposite arm to the administration site. At each timepoint, approximately 1 mL of blood was drawn, and the activity was determined using a calibrated gamma counter. Blood count values obtained for each patient were decay corrected with respect to the sampling time and average values per collection timepoint for cohort A were used for PK curve fitting using the two-compartmental model for IV bolus injection of the PKSolver tool [19].

2.8. Biodistribution and preliminary imaging findings

Healthy organs and primary, nodal, and metastatic lesions were visually assessed at each timepoint. Areas of unexpected uptake were further investigated if management could be influenced according to clinical judgement. Additionally, semiquantitative evaluations were performed by means of SUV_{max} and SUV_{mean} at all timepoints (i.e., immediately after the administration, and at 10, 20, 60, and 120 min post injection).

2.9. Image quality

To determine the optimal timepoint for image acquisition for future studies, we assessed lesion:reference organ ratio at each timepoint. As reference organs, heart as surrogate for the blood pool as well as muscle and healthy organs corresponding to the site of tumor lesions were considered. Reconstruction of the list mode datasets with an undersampling of counts simulating lower administered activities (200, 150, 100, and 50 MBq) was performed to evaluate if lower administered activities could yield suitable image quality for future applications. Each reconstructed dataset, as well as the original scan at the corresponding timepoint, have been evaluated according to the qualitative 5-points Likert scale, by two investigators (FG and MK) to assess: i) noise (1 no noise → 5 extremely noisy), ii) lesion to background contrast (1 excellent contrast → 5 no contrast between lesion and background), iii) diagnostic confidence (1 excellent diagnostic confidence → impossible to take a diagnostic decision).

3. Results

3.1. Patient characteristics

A total of 19 patients were screened, and 18 patients (12 female, 6 male) were included in this study between November 2023 and April 2024. All enrolled patients received a single administration of around 250 MBq [68Ga]Ga-OncoFAP (mean activity: 239.7 ± 23.7 MBq, range 178–274 MBq) and were therefore included in the safety evaluation. Patient age ranged from 45 to 76 years (median, 57 years). Three (3) male and three (3) female patients were enrolled in cohort A, while an additional nine female and three male patients were enrolled in cohort B. Details on the patient characteristics are depicted in Table 1.

3.2. Safety

No serious adverse events occurred during the study. Only one (1) patient out of 18 experienced a single adverse event, a transient Grade 1 headache after the end of the last PET/CT scan. No action was taken due to the adverse event, and the headache resolved on the same day. The attending physician evaluated the adverse event as not related to the study drug but assessed tiredness as cause of the headache. Thus, no [68Ga]Ga-OncoFAP-related adverse events were reported. No clinically significant changes to serum chemistry, hematology, coagulation, vital signs, physical examination, and ECG were recorded in any of the patients participating in this study. An overview of the number of adverse events (AEs), including serious adverse events, and treatment-related adverse events is depicted in Table 2.

3.3. Dosimetry

The dosimetry results for each organ as well as the effective dose are depicted in Table 3. The effective dose per patient ranged from 16.6 to 24.6 mSv/GBq (mean 19.9 mSv/GBq, median 19.4 mSv/GBq). The organs absorbing the highest doses were the urinary bladder wall (70.1–132 mGy/GBq), kidneys (18.9–49.3 mGy/GBq) and small intestine (12.8–28.8 mGy/GBq). The effective dose was higher for female patients (20.2–24.6 mSv/GBq) than for male patients (16.6–18.6 mSv/GBq), most likely due to uptake in the uterus (16.7–17.3 mGy/GBq) and ovaries (16.1–16.2 mGy/GBq), which were higher than the absorbed dose in the testes (10.3–11.6 mGy/GBq).

3.4. Pharmacokinetics

Maximum serum concentration (C_{max}) was reached within 1 min for most patients, and the half-life of the alpha phase ($t_{1/2}\alpha$) is estimated to be 0.9 min, while the half-life of the beta phase ($t_{1/2}\beta$) is around 36 min. The area under the curve ($AUC_{0\text{-}t}$) is estimated to be 1013 kBq/mL*min. Average values for both cohorts and individual patients are depicted in Fig. 2 together with the curve fitting.

3.5. Biodistribution and preliminary imaging findings

Based on the imaging and dosimetry results, it was determined that the elimination of [68Ga]Ga-OncoFAP is predominantly kidney-mediated as a signal was observed in the renal pelvis and bladder shortly after administration, while no time-dependent accumulation in liver, bile duct, or intestines was seen (Fig. 4). Tumor uptake was observed shortly after administration, with median SUV_{max} equal to 9.44, ranging from 1.99 to 31.36 in cohort A and median 9.4 (range, 4.02–18.3) in cohort B. The biodistribution in terms of SUV_{mean} in the tumor and healthy organs is shown in Fig. 3 at different timepoints. There was considerable variability between the lesions which is most likely related to the biology and size of the different lesions. In most healthy organs such as bone, brain, lungs, stomach, colon, and skin, low uptake was observed at all timepoints. By contrast, a reduction over time was observed in organs such as the heart, liver, kidneys, and small intestine. There was a significant patient-to-patient variability in uptake in the normal pancreas. Uptake values at different timepoints are reported in the Supplementary Table 1–6.

Representative maximum intensity projections are depicted in Fig. 4. Overall, all previously known lesions were also detected during the [68Ga]Ga-OncoFAP PET/CT scan. For one treatment-naïve patient affected by upper outer quadrant breast cancer (cT1ccN0cM0), the [68Ga]Ga-OncoFAP PET/CT scan revealed an additional suspicious

Table 1
Disposition of patients and baseline characteristics per cohort and overall.

		Cohort A		Cohort B		Total	
		(n = 6)		(n = 12)		(N = 18)	
Disposition of patients	Enrolled	6	100 %	12	100 %	18	100 %
	Safety Evaluable	6	100 %	12	100 %	18	100 %
	Treated	6	100 %	12	100 %	18	100 %
Tumor type	Pancreatic	3	50 %	2	17 %	5	28 %
	Breast	1	17 %	7	58 %	8	44%
	Esophageal	2	33 %	1	8 %	3	17 %
	Colorectal	0	0%	2	17 %	2	11%
Indication	Initial staging	5		4		9	50 %
	Restaging	1		8		9	50 %
Age	Mean		64.2		59.8		61.3
	SD		12.46		11.32		11.53
	Min		48		45		45
	Max		76		76		76
	Median		69		56		57
Gender	Female	3	50 %	9	75 %	12	67 %
	Male	3	50 %	3	25 %	6	33 %
Weight (kg)	Mean ± Sd	69.2 ± 21.1		61.5 ± 12.8		64.1 ± 15.8	
	[Min-Max]	[55–110]		[40–77.5]		[40–110]	
	Median	60.5		61.5		61.5	
ECOG[1]:	0	5	83 %	11	92 %	16	89 %
	1	1	17 %	1	8 %	2	11 %
Prior anti-cancer chemotherapy	Neo-adjuvant	0	0 %	3	25 %	3	17 %
	Unknown	0	0 %	3	25 %	3	17 %
	Metastatic	0	0 %	2	17 %	2	11%
	Locally advanced	1	17 %	0	0 %	1	6%
	Adjuvant	0	0%	3	25 %	3	17 %
	Overall	1	17 %	8	67 %	9	50 %
Prior anti-cancer radiotherapy		0	0 %	4	33 %	4	22%
Prior anti-cancer surgery (incl. biopsy)		4	67 %	11	92 %	15	83 %

ECOG - Eastern Cooperative Oncology Group Performance Status Scale; SD – standard deviation.

Table 2
Overview of adverse events.

	Overall	Grade 1	Grade 2	Grade 3	Grade 4
Serious adverse events	0	0	0	0	0
Drug-related adverse event	0	0	0	0	0
Adverse event	1	1	0	0	0

nodule in the right breast (SUV_{max} = 22.14, SUV_{mean} = 15.16, and T/B ratio = 6 at 60 min). The lesion was removed during the pre-planned surgery to remove the previously known lesion and subsequent histological analysis confirmed the presence of infiltrating carcinoma in the upper quadrant of the right breast. In two additional patients, new suspected lesions were discovered based on the [^{68}Ga]Ga-OncoFAP PET/CT, but these were not confirmed by histopathology as no change to the patient management was foreseen based on these additional lesions. Representative images are shown in Fig. 5.

3.6. Image quality

The highest tumor:heart ratio was observed at 1 h post administration and at this timepoint, the uptake in healthy organs such as colon, liver, lung, muscle, small intestine, and spleen also tended to be slightly lower than at earlier timepoints. Tumor uptake up to the 2 h timepoint was relatively stable. The assessments of image quality on images simulating lower administered activities (e.g., ca 200, 150, 100, and 50 MBq), demonstrated good contrast, low level of noise, and good diagnostic confidence for images with activities of 150 and 200 MBq.

4. Discussion and conclusion

The Phase I clinical trial described in this report is the first prospective study evaluating the safety and dosimetry of the novel diagnostic radiopharmaceutical [^{68}Ga]Ga-OncoFAP in patients with cancer.

No serious adverse events or drug-related adverse events were observed in this study. The favorable safety profile of [^{68}Ga]Ga-OncoFAP in 18 patients receiving an administration of 178–274 MBq [^{68}Ga]Ga-OncoFAP is in line with other diagnostic radiopharmaceuticals. Due to the low mass amount of tracer administered and the relatively low amount of radioactivity, adverse events for diagnostic radiopharmaceuticals are rare. Accordingly, no treatment-related adverse events were recorded in this study.

The effective dose of around 20 mSv/GBq is within the typical range of the doses of other frequently used diagnostic radiopharmaceuticals and does not pose any concerns related to radiation protection [20]. The organs absorbing the highest doses were the urinary bladder wall (70.1–132 mGy/GBq) and kidneys (18.9–49.3 mGy/GBq), related to the urinary excretion of the radiopharmaceutical. Our results are consistent with previous studies that reported the median effective dose for the [^{68}Ga]Ga-labelled and [^{18}F]F-labelled radiopharmaceuticals of 0.0123 mSv/MBq and of 0.0141 mSv/MBq, respectively, when using an activity of 100–200 MBq [21]. The effective dose was higher for female than for male patients (20.2–24.6 mSv/GBq and 16.6–18.6 mSv/GBq, respectively), most likely due to the higher uptake recorded in the uterus, which exhibits physiological FAP expression [22], and ovary, which summed was more than double the absorbed dose at the testes. Therefore, based on the safety signals and dosimetry evaluation, [^{68}Ga]Ga-OncoFAP is considered safe for implementation in future clinical trials.

Based on preclinical findings [10] and results with similar tracers [21], [^{68}Ga]Ga-OncoFAP showed a favorable biodistribution profile at early timepoints after administration. There was a significant patient-to-patient variability in uptake in the normal pancreas. We can speculate that this finding might be related to inflammatory changes, as already shown for other FAP-targeting compounds [23], which can lead to FAP expression in patients affected by pancreatic cancer (5/18

Table 3
Individual dosimetry estimates for the three male and three female patients included in the dosimetry analysis (Cohort A). As five out of six patients had a lesion close to the pancreas, the values of only one patient were considered to calculate the dose to the pancreas. LLI = Lower Large Intestine, ULI = Upper Large Intestine.

Patient sex		M	M	M	F	F	F
Injected Activity [MBq]		234	192	239	274	240	258
Dose [mGy/GBq]	Adrenals	12.3	11.9	10.6	15.6	15.9	15.9
	Brain	2.2	2.39	2.19	4.03	3.72	3.53
	Breasts	10.4	9.97	8.73	12.9	12.9	13.4
	Gallbladder Wall	12.5	12.1	10.7	15.1	15.9	15.3
	LLI Wall	13.4	13.1	12.2	15.9	16	16.5
	Small Intestine	12.9	18.2	19.6	28.8	23.8	–
	Stomach Wall	15.9	13.1	14.7	20	20.5	18.4
	ULI Wall	12.7	12.4	11.2	15.7	15.8	15.9
	Heart Wall	12.2	11.6	13.7	28.5	20.6	18.8
	Kidneys	20.4	18.9	28.8	49.3	36.8	47.1
	Liver	13.2	8.57	9.54	20.5	28.5	14.4
	Lungs	25.1	23.9	23.5	52.4	32.9	35.6
	Muscle	11.5	11	9.81	13.7	13.9	14.4
	Ovaries	–	–	–	16	16.1	16.5
	Pancreas	–	–	–	–	–	18.7
	Red Marrow	10.9	10.7	10.2	14.1	12.8	14.5
	Osteogenic Cells	17	16.4	14.8	23.4	22.5	24.6
	Skin	10	9.61	8.42	11.9	12.1	12.6
	Spleen	13.3	11.6	15.7	21.2	18.7	17.3
	Testes	11.9	11.5	10.4	–	–	–
	Thymus	11.6	11.2	9.89	14.7	14.6	15.1
	Thyroid	11.4	11	9.5	13.1	13.4	14
	Urinary Bladder Wall	70.1	98.5	132	108	106	69
	Uterus	–	–	–	16.9	17	17.4
	Total Body	12.1	11.9	10.9	15.6	15.7	15.4
[mSv/GBq]	Effective Dose	16.6	17.2	18.6	24.6	22.4	20.2

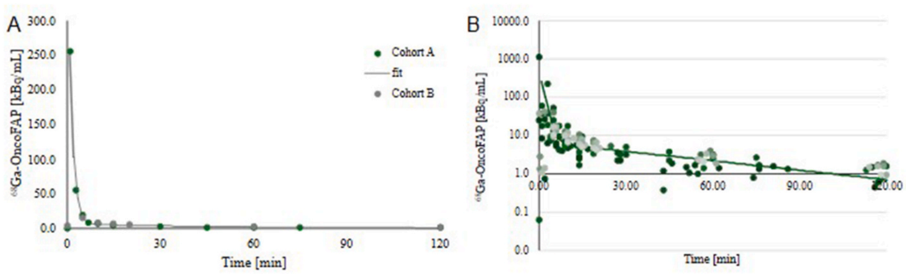

Fig. 2. Pharmacokinetics of [^{68}Ga]Ga-OncoFAP (A) average values for cohort A and B as well as the curve fitting (B) individual patient data and the curve fitting.

patients in this study). Additionally, these results might be related to the high FAP expression in Langerhans islets [24], which might vary among patients.

For reproducibility of uptake evaluation, all centers used PET/CT scanners that received EARL accreditation with gallium-68 radioisotope. Currently, there is no consensus on the acceptable reference organs or on a qualitative uptake scale (mild, moderate, intense) [21]. In our cohort, tumor lesions were found with SUV_{max} ranging from 1.99 to 31.36, 4.16 to 21.52, and 5.04 to 21.7 at the initial, 60 min, and 120 min scans, respectively. The most stable uptake over time was seen in bone, brain, lungs, stomach, colon, and skin. For future investigations, computing the lesion:reference organ ratio with respect to these organs might be considered. The choice between SUV and ratio evaluation should be further clarified in future clinical trials.

Since rapid and selective accumulation in tumor lesions as well as fast clearance from the circulation and healthy organs were observed, reasonably good imaging quality could be obtained shortly after administration (10–20 min post injection). However, the tumor:organ ratio was highest at 1–2 h after administration. Therefore, in the future, scans will most likely be acquired at around 1 h post administration. This uptake time, consistent with that reported for other FAP-targeting PET compounds labelled with gallium-68 in the procedural EANM/SNMMI guidelines [21], also aligns with that of other radiopharmaceuticals commonly used in clinical practice (e.g. [^{18}F]FDG and ^{68}Ga-labelled SSTR analogues). Based on simulations of lower administered activities at around 1 h post-administration, it could be concluded that an administered activity of around 150 MBq would be suitable for future applications. Timing and activity may be adjusted according to the clinical setting. Our results are in line with the procedural EANM/SNMMI guidelines that recommend an administered activity of 100–200 MBq for gallium-68 compounds when using conventional PET cameras, and half of the advised activity for digital total-body scanners [21].

FAP-targeting diagnostic radiopharmaceuticals are promising new imaging modalities which may improve staging and restaging in different types of cancer [6–8]. [^{68}Ga]Ga-OncoFAP seems to fit in this landscape as it showed very promising properties as diagnostic radiopharmaceutical in terms of rapid and selective accumulation in tumor lesions and fast clearance from healthy organs. While this study was not designed and powered to evaluate the diagnostic performance in terms of sensitivity and specificity, encouraging initial results were obtained as all previously known lesions were detected by the [^{68}Ga]Ga-OncoFAP PET/CT scan. This was expected since we enrolled patients with solid tumors characterized by intense desmoplastic reaction (pancreatic, colorectal, breast, and esophageal cancers), which highly express FAP [25–27]. Additionally, for three patients, previously unknown putative lesions were detected with [^{68}Ga]Ga-OncoFAP PET/CT. For one of those patients, the new lesion was surgically removed and confirmed as true

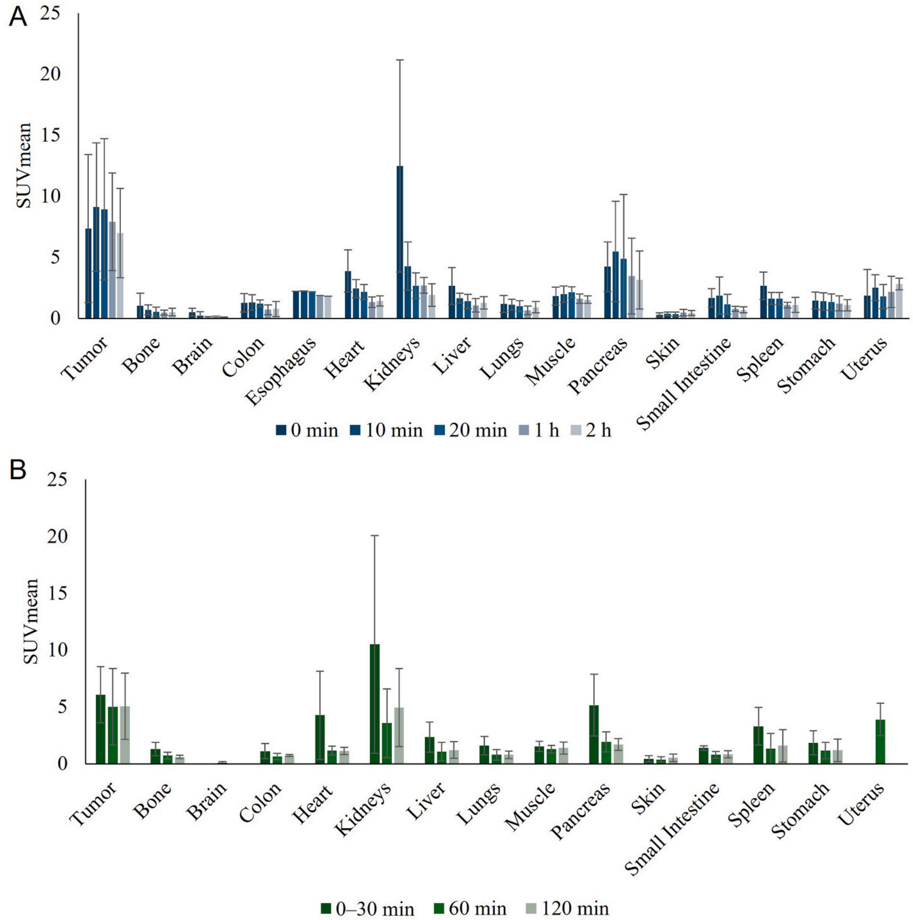

Fig. 3. Biodistribution in terms of SUV_{mean} in the tumors and healthy organs for cohort A (A) and cohort B (B). Timepoints represent the planned start time of the scan and are indicative only, as slight delays in acquisition time occasionally occurred.

positive for breast cancer by histology. For the other two patients, the management would not be changed based on the identity of the newly discovered putative lesions and therefore no further investigations were carried out. Although preliminary and based on a small cohort, these findings suggest that [^{68}Ga]Ga-OncoFAP could have a substantial clinical impact on management of oncologic patients, potentially upstaging the disease. Several studies with other diagnostic FAP ligands showed that these ligands have a superior diagnostic performance compared to standard of care modalities [6–8]. Even though this study was not powered to evaluate diagnostic performance, these findings are encouraging for future development. Moreover, FAP is overexpressed in fibroblasts activated in multiple non-oncological conditions, such as inflammation, wound healing, and fibrosis. Consequently, FAP-targeting PET has the potential to be applied in both oncological and non-oncological diseases [28].

We acknowledge some limitations of our study. We did not perform analyses to assess the diagnostic accuracy of the [^{68}Ga]Ga-OncoFAP PET/CT nor a comparison with other radiopharmaceuticals PET/CT or conventional imaging modalities. However, these objectives were out of scope of the present phase I study. Future studies aimed at investigating the diagnostic performance of [^{68}Ga]Ga-OncoFAP in defined clinical settings and to refine technical parameters are planned.

In conclusion, the results of the Phase I trial demonstrate a favorable safety profile of [^{68}Ga]Ga-OncoFAP with an effective dose commensurate with that of other diagnostic radiopharmaceuticals. [^{68}Ga]Ga-OncoFAP exhibited optimal pharmacokinetics and demonstrated promising PET imaging of a range of solid tumors. The rapid and selective accumulation of [^{68}Ga]Ga-OncoFAP in tumor lesions supports imaging at early timepoints. Highest tumor:reference organ ratios were observed at 1 h, so imaging in this timeframe is also supported. Since the tumor:reference organ did not significantly change between 1 and 2 h, the optimal imaging timepoint is most likely 1 h due to convenience for patients and caregivers. Based on the results obtained in this study, activities of around 150 MBq were deemed suitable for future applications. Preliminary efficacy results are also encouraging and warrant the conduct of future studies to explore the diagnostic performance of [^{68}Ga]Ga-OncoFAP in defined settings.

CRediT authorship contribution statement

Margarita Kirienko: Writing – review & editing, Writing – original draft, Investigation, Data curation. **Martina Sollini:** Writing – review & editing, Writing – original draft, Investigation, Data curation. **Emanuele Balduzzi:** Writing – review & editing, Writing – original draft, Formal analysis, Data curation. **Alessia Artesani:** Writing – review & editing, Methodology, Formal analysis. **Elena Lazzeri:** Writing – review & editing, Investigation. **Fabrizia Gelardi:** Writing – review & editing, Investigation. **Francesco Bartoli:** Writing – review & editing, Methodology, Investigation, Conceptualization. **Andrea Marciano:** Writing – review & editing, Investigation. **Paola Caroli:** Writing – review & editing, Investigation. **Samuele Cazzamalli:** Writing – review & editing, Writing – original draft, Methodology, Conceptualization. **Andrea Galbiati:** Writing – review & editing, Conceptualization. **Jacqueline Mock:** Writing – review & editing, Writing – original draft, Project administration, Methodology, Formal analysis, Conceptualization. **Dario Neri:** Writing – review & editing, Writing – original draft, Resources, Methodology, Conceptualization. **Marco Maccauro:** Writing – review & editing, Investigation, Data curation. **Federica Matteucci:**

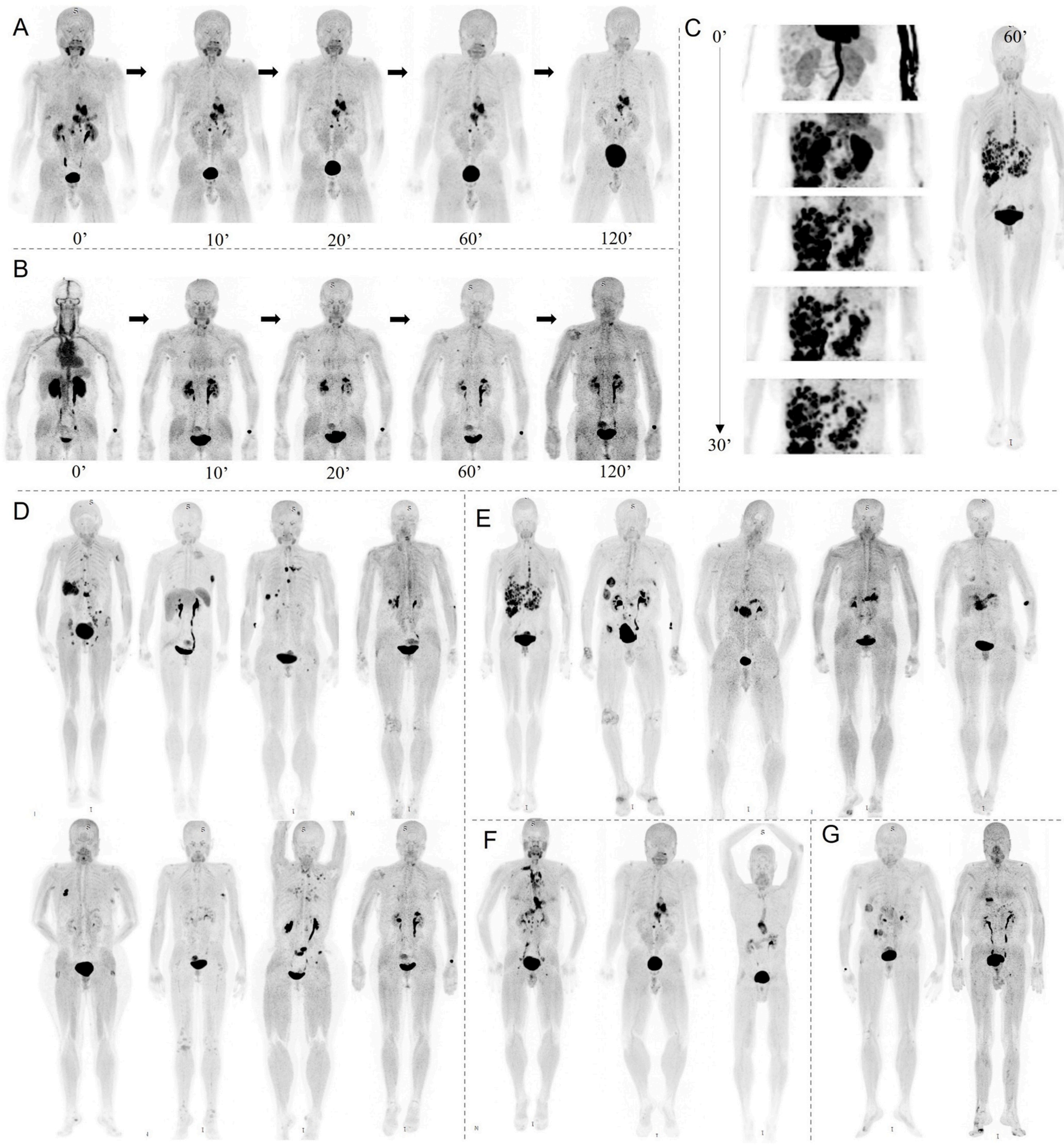

Fig. 4. Representative maximum intensity projections of a male cohort A patient with esophageal cancer (A), a female cohort A patient with pancreatic cancer (B), a cohort B patient with pancreatic cancer (C), the breast cancer (D), pancreatic cancer (E), esophageal cancer (F) and colorectal cancer patients (G) D-G were acquired at 1 h post-administration. Timepoints are indicative as slight delays in acquisition time occasionally occurred.

Writing – review & editing, Investigation, Data curation. **Pinuccia Faviana:** Writing – review & editing, Investigation, Data curation. **Arturo Chiti:** Writing – review & editing, Writing – original draft, Investigation, Conceptualization. **Paola Anna Erba:** Writing – review & editing, Writing – original draft, Methodology, Formal analysis, Conceptualization.

Other disclosures

This study has been approved by the Ethics Committee Comitato Etico Territoriale Lazio Area 5 (CTIS ID 931, 04/10/2022) and national competent authorities. All patients signed an informed consent form.

Disclosure

Please fill in all the relevant sections below. If/wherever necessary, please state "Not applicable".

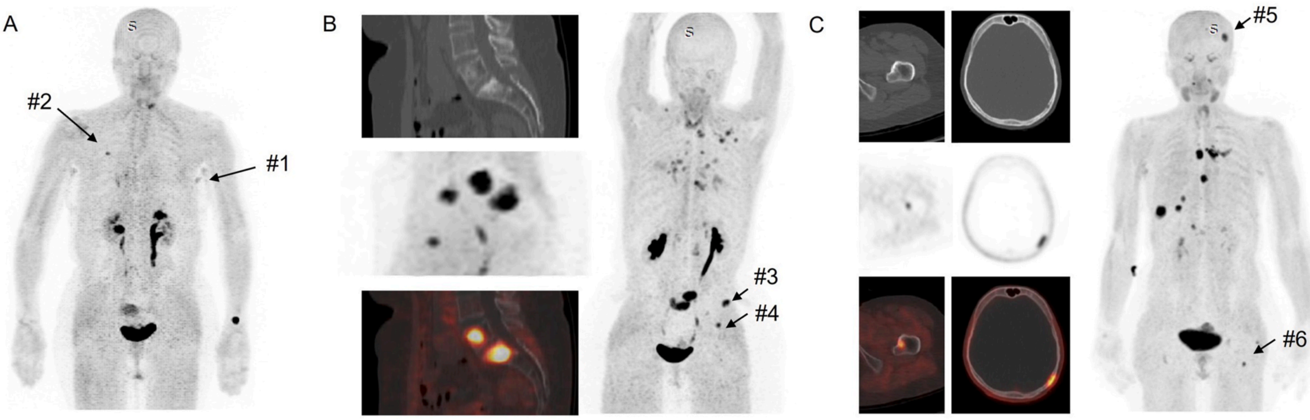

Fig. 5. Representative images of patients in whom additional lesions were detected (A) treatment-naïve breast cancer initially diagnosed with T1c N0 M0 breast cancer in the upper outer quadrant of the left breast, the [^{68}Ga]Ga-OncoFAP-PET/CT scan revealed the known primary lesion in the left breast (#1) as well as an additional suspected nodule in the right breast (#2), which was later confirmed as invasive carcinoma (B) breast cancer patient initially diagnosed with stage T2 N1 M0 invasive carcinoma of the left breast, which was treated with initial surgery followed by adjuvant chemotherapy and tamoxifen and a second surgery followed by adjuvant exemestane, stage at screening: Tx N3 M0, the [^{68}Ga]Ga-OncoFAP-PET/CT scan revealed previously unknown, suspected lesions in the hip bone (#3 & #4) in addition to the known lymph node lesions (C) breast cancer patient initially diagnosed with stage T1 N3 M0 invasive carcinoma of the left breast which was treated with neoadjuvant paclitaxel and epirubicin + cyclophosphamide followed by surgery as initial treatment, followed by exemestane treatment, stage at screening: Tx Nx M1, the [^{68}Ga]Ga-OncoFAP-PET/CT scan revealed additional, previously unknown suspected lesions in the skull and femur (#5 & #6).

Study methodology

State the nature of the study:

- prospective
- multicentre
- open label
- Phase I
- diagnostic

Institutional review board approval

This study has been approved by the Ethics Committee Comitato Etico Territoriale Lazio Area 5 and national competent authorities.

Written informed consent

All patients signed an informed consent form.

Ethical standards

For studies involving animal data:

Ethics Commitee approval CTIS ID 931, 04/10/2022 (no animals were involved in the research described in this article).

Clinical trial registration

The study's clinical trial registration number is NCT05784597 registered with Clinicaltrials.gov and 2022-500902-16-00 registered with EuCT.

Funding

The study presented in this article was funded in its entirety by the Sponsor Philogen S.p.A.

Declaration of competing interest

Please declare here any financial or non-financial competing interests. Use authors' initials when declaring each author's competing interests.

SC, AG and JM are employees of Philochem AG. DN is a founder and shareholder of Philogen S.p.A. MS received speaker honoraria from Elma academy, Train srl, Accademia nazionale di medicina and GE healthcare. Furthermore, MS is an Associate Editor of Cancer Imaging for the “Artificial intelligence, machine learning and radiomics” section.

AC is the Editor in Chief of The EANM Journal but was not involved in any way in the evaluation, revision, or decision process of this article.

AC declares the following competing interests: Consulting or advisory role.

- *Blue Earth Diagnostics*
- *Telix Pharmaceuticals*
- *InnovaRadi Therapeutic*

Speaker's Bureau.

- *Bracco Diagnostics*
- *General Electric*
- *Novartis*
- *Telix Pharmaceuticals*
- *United Imaging*

PAE received an unrestricted educational grant from Pfizer. PF and FB are consultants for Philochem AG and Philogen S.p.A. PAE reports research contracts with Philogen, Immedica.

Acknowledgements

We acknowledge the support from the investigators at Fondazione IRCCS Istituto Nazionale dei Tumori: Medical Oncology Department coordinated by Prof. de Braud, and the collaboration of Dr. Di Nicola Massimo, Pietrantonio Filippo, Bianchi Giulia, Capri Giuseppe, Vernieri Claudio, Niger Monica, Duca Matteo, Cresta Sara, Damian Silvia; Nuclear Medicine Department - Technologists – Matteo Ragazzoni, Monica Testoni, Marco Magistretti; Medical Physicist – Carlo Chiesa, Nurses – Rita Sicari, Aurelio, Peny, Calogero, Riccardo; Radiopharmacists – Claudio Pascali, Anna Bogni and Data manager – Maria Libera La Porta. We acknowledge the support from the investigators at IRCCS Ospedale San Raffaele: Medical Oncologists and Surgeons – Prof. Reni, Prof. Falconi, Prof. Gentilini, Prof. Rosati, Radiopharmacists - Maria Grazia Minotti, Silvia Debbia, Valeria Masiello, Angela Coliva, Technologists –

Giuseppe Bonfitto, Serena Pincherri, Raffaele Menichini, Medical Physicists – Annarita Savi, Michela Olivieri, Nurse – Rita Petrelli, and Data manager – Di Donato Rachele. We acknowledge the support from the investigators at Regional Center of Nuclear Medicine, Azienda Ospedaliero Universitaria Pisana: Medical Oncology Department – Andrea Fontana; Technologists – Kinzika Ruggiero, Marco Lessi; Nurses – Calogero Bartolotta, Federica Roas. We acknowledge the support from the investigators at IRCCS Istituto Romagnolo per lo Studio dei Tumori "Dino Amadori" - IRST S.r.l.: Nuclear Medicine Departement –Paola Caroli, Monica Celli, Lorenzo Fantini, Federica Matteucci; Technologists – Valentina Migani, Maria Caternicchia, Valentina Mautone, Gianina Volpe, Daniela Migani; Medical Physicist – Anna Sarnelli, Maria Luisa Belli; Radiopharmapharmacist - Valentina Di Iorio; Nurses – Carmela Lamberti, Monica Golinucci; Data managers – Lucia Fabbri, Manuela Monti.

Appendix A. Supplementary data

Supplementary data to this article can be found online at https://doi.org/10.1016/j.eanmj.2025.100013.

Data availability

Data will be made available on request.

References

[1] Kelly T, Huang Y, Simms AE, Mazur A. Fibroblast activation protein-alpha: a key modulator of the microenvironment in multiple pathologies. Int Rev Cell Mol Biol 2012;297:83–116.
[2] Kirienko M, Gelardi F, Fiz F, Bauckneht M, Ninatti G, Pini C, et al. Personalised PET imaging in oncology: an umbrella review of meta-analyses to guide the appropriate radiopharmaceutical choice and indication. Eur J Nucl Med Mol Imag 2024;52(1): 208–24.
[3] Siegel RL, Miller KD, Fuchs HE, Jemal A. Cancer Statistics, 2021. CA Cancer J Clin 2021;71(1):7–33.
[4] Rettig WJ, Garin-Chesa P, Beresford HR, Oettgen HF, Melamed MR, Old LJ. Cell-surface glycoproteins of human sarcomas: differential expression in normal and malignant tissues and cultured cells. Proc Natl Acad Sci U S A 1988;85(9):3110–4.
[5] Jansen K, Heirbaut L, Verkerk R, Cheng JD, Joossens J, Cos P, et al. Extended structure-activity relationship and pharmacokinetic investigation of (4-quinolinoyl)glycyl-2-cyanopyrrolidine inhibitors of fibroblast activation protein (FAP). J Med Chem 2014;57(7):3053–74.
[6] Kratochwil C, Flechsig P, Lindner T, Abderrahim L, Altmann A, Mier W, et al. (68) Ga-FAPI PET/CT: tracer uptake in 28 different kinds of cancer. J Nucl Med 2019;60 (6):801–5.
[7] Sollini M, Kirienko M, Gelardi F, Fiz F, Gozzi N, Chiti A. State-of-the-art of FAPI-PET imaging: a systematic review and meta-analysis. Eur J Nucl Med Mol Imag 2021;48(13):4396–414.
[8] Treglia G, Muoio B, Roustaei H, Kiamanesh Z, Aryana K, Sadeghi R. Head-to-Head comparison of Fibroblast Activation Protein Inhibitors (FAPI) radiotracers versus [(18)F]F-FDG in oncology: a systematic review. Int J Mol Sci 2021;22(20).
[9] Wass G, Clifford K, Subramaniam RM. Evaluation of the diagnostic accuracy of FAPI PET/CT in oncologic studies: systematic review and metaanalysis. J Nucl Med 2023;64(8):1218–24.
[10] Millul J, Bassi G, Mock J, Elsayed A, Pellegrino C, Zana A, et al. An ultra-high-affinity small organic ligand of fibroblast activation protein for tumor-targeting applications. Proc Natl Acad Sci U S A 2021;118(16).
[11] Backhaus P, Gierse F, Burg MC, Buther F, Asmus I, Dorten P, et al. Translational imaging of the fibroblast activation protein (FAP) using the new ligand [(68)Ga] Ga-OncoFAP-DOTAGA. Eur J Nucl Med Mol Imag 2022;49:1822–32.
[12] Bartoli F, Elsinga P, Nazario LR, Zana A, Galbiati A, Millul J, et al. Automated radiosynthesis, preliminary In Vitro/In vivo characterization of OncoFAP-Based radiopharmaceuticals for cancer imaging and therapy. Pharmaceuticals 2022;15 (8).
[13] Stabin MG, Sparks RB, Crowe E. OLINDA/EXM: the second-generation personal computer software for internal dose assessment in nuclear medicine. J Nucl Med 2005;46(6):1023–7.
[14] Wasserthal J, Breit HC, Meyer MT, Pradella M, Hinck D, Sauter AW, et al. TotalSegmentator: robust segmentation of 104 anatomic structures in CT images. Radiol Artif Intell 2023;5(5):e230024.
[15] Kletting P, Kull T, Reske SN, Glatting G. Comparing time activity curves using the Akaike information criterion. Phys Med Biol 2009;54(21):N501–7.
[16] Sgouros G. Bone marrow dosimetry for radioimmunotherapy: theoretical considerations. J Nucl Med 1993;34(4):689–94.
[17] Hindorf C, Glatting G, Chiesa C, Linden O, Flux G, Committee ED. EANM Dosimetry Committee guidelines for bone marrow and whole-body dosimetry. Eur J Nucl Med Mol Imag 2010;37(6):1238–50.
[18] Stabin MG. MIRDOSE: personal computer software for internal dose assessment in nuclear medicine. J Nucl Med 1996;37(3):538–46.
[19] Zhang Y, Huo M, Zhou J, Xie S. PKSolver: an add-in program for pharmacokinetic and pharmacodynamic data analysis in Microsoft Excel. Comput Methods Progr Biomed 2010;99(3):306–14.
[20] Quinn B, Dauer Z, Pandit-Taskar N, Schoder H, Dauer LT. Radiation dosimetry of 18F-FDG PET/CT: incorporating exam-specific parameters in dose estimates. BMC Med Imag 2016;16(1):41.
[21] Hope TA, Calais J, Goenka AH, Haberkorn U, Konijnenberg M, McConathy J, et al. SNMMI Procedure Standard/EANM Practice Guideline for Fibroblast Activation Protein (FAP) PET. J Nucl Med 2025;66(1):26–33.
[22] Zhang X, Song W, Qin C, Song Y, Liu F, Hu F, et al. Uterine uptake of 68Ga-FAPI-04 in uterine pathology and physiology. Clin Nucl Med 2022;47(1):7–13.
[23] Rohrich M, Naumann P, Giesel FL, Choyke PL, Staudinger F, Wefers A, et al. Impact of (68)Ga-FAPI PET/CT imaging on the therapeutic management of primary and recurrent pancreatic ductal adenocarcinomas. J Nucl Med 2021;62(6):779–86.
[24] Kirienko M, Centonze G, Sabella G, Sollai M, Sollini M, Lan X, et al. FAP expression in alpha cells of Langherhans insulae-implications for FAPI radiopharmaceuticals' use. Eur J Nucl Med Mol Imag 2023;50(10):3042–9.
[25] Whatcott CJ, Diep CH, Jiang P, Watanabe A, LoBello J, Sima C, et al. Desmoplasia in primary tumors and metastatic lesions of pancreatic cancer. Clin Cancer Res 2015;21(15):3561–8.
[26] Backhaus P, Burg MC, Roll W, Buther F, Breyholz HJ, Weigel S, et al. Simultaneous FAPI PET/MRI targeting the fibroblast-activation protein for breast cancer. Radiology 2022;302(1):39–47.
[27] Elboga U, Sahin E, Kus T, Cayirli YB, Aktas G, Uzun E, et al. Superiority of (68)Ga-FAPI PET/CT scan in detecting additional lesions compared to (18)FDG PET/CT scan in breast cancer. Ann Nucl Med 2021;35(12):1321–31.
[28] Busek P, Mateu R, Zubal M, Kotackova L, Sedo A. Targeting fibroblast activation protein in cancer - prospects and caveats. Front Biosci (Landmark Ed) 2018;23(10): 1933–68.